Polymer Chemistry

Accepted Manuscript

ROYAL SOCIETY OF CHEMISTRY

www.rsc.org/polymers

Journal Name

RSCPublishing

ARTICLE

Synthesis and Characterization of Regiorandom Homopolymer of 3-Alkyldithieno[3,2-*b*:2',3'-*d*]thiophene for Thin-Film Transistors

Fei Wang,[a] Gongqiang Li,[a] Dongchen Qi,[b] Ivy Wong Hoi Ka[a] and Jun Li[a]

Cite this: DOI: 10.1039/xoxxoooooox

Received ooth January 2012,
Accepted ooth January 2012

DOI: 10.1039/xoxxoooooox

www.rsc.org/

Regiorandom homopolymer of 3-alkyldithieno[3,2-*b*:2',3'-*d*]thiophene (P3ADTT) has been prepared by oxidative polymerization using Iron(III) Chloride and oxygen as oxidants. Physical and electrochemical properties of the homopolymer were investigated and compared with these of P3HT. Its application in organic field-effect transistors showed annealing-free hole mobility up to 0.048 $cm^2/V \cdot s$ at room temperature and great thermally stable mobility of 0.13 $cm^2/V \cdot s$ at 200 °C with current on/off ratio of greater than 10^5.

Introduction

With the advantage of convenient solution processability, organic semiconducting polymers[1, 2] have been extensively studied and are considered as promising alternative to hydrogenated amorphous silicon material for their potential application in large-area, light weight and mechanically flexible electronics such as organic light-emitting diodes (OLEDs), organic photovoltaic (OPV),[3-6] and organic thin-film transistors (OTFTs).[7-9]

As prototypical semiconducting material - polythiophene is insoluble, soluble thiophene-based polymers, in which alkyl side chains are introduced into thiophene backbone to enhance solubility, have been developed. Regioregular poly(3-hexylthiophene) (P3HT)[10-14] is the most studied one among this class of materials. With the help of regioregular alkyl chains, polymer chains are packed more efficiently and held in coplanarity. Up to 0.1 $cm^2/V \cdot s$ field-effect hole mobility has been reported.[15] However, large extend of π-conjugation in regioregular P3HT also results in high-lying HOMO energy level (small ionization potential) which makes the material prone to photoinduced oxidation.[16]

Using fused thiophene ring instead of single thiophene ring is an efficient strategy for obtaining higher charge carrier mobility.[17-19] Fused-ring unit may significantly lower the HOMO level which leads to better oxidative stability of the devices. Moreover, fused ring unit with larger planarity can improve the polymer backbone chain packing and thus promote the formation of large crystalline domains in solid state, leading to better intermolecular charge transfer. However, fused ring unit can also decrease the solubility of the polymer. Thus optimization for the ring number of fused unit and selection of suitable side chain are crucial to achieve good hole mobility.[20, 21]

Among varieties of fused thiophene units, dithieno[3,2-*b*:2',3'-*d*]thiophene (DTT),[22] consisting of three fused thiophene rings, is one of the most intensively studied building blocks for the construction of electronically useful semiconducting small molecules[23-25] and copolymers.[26-31] As example of OTFT application, high hole mobility (0.42 $cm^2/V \cdot s$) was reported for DTT-based small molecule, in which DTT moiety was end-capped by phenyl group.[24] Examples of DTT-based copolymers for OTFT application are limited. Copolymer incorporating unsubstituted DTT and 2,6-bis(3-alkylthiophene) reported by us in 2008 exhibited the highest mobility (0.3 $cm^2/V \cdot s$, on/off ratio of over 10^7) among all the DTT-based polymers reported at that time.[32] Hole mobility up to 0.60 $cm^2/V \cdot s$ for polymer based on DTT and diketopyrrolopyrrole was reported in 2012.[33] But despite that doped poly unsubstituted DTT were electrochemically synthesized in 1985,[34, 35] the only example on homopolymers of substituted DTT monomers was report by Zhang *et al.* in 2009.[36] They synthesized and characterized poly(3,5-didecanyldith-ieno[3,2-*b*:2',3'-*d*]thiophene) but no electronic application was demonstrated due to the poor absorption of the homopolymer. Considering that instructive information will surely be obtained from the characteristic comparison between polythiophene and DTT homopolymer, research work on DTT-based homopolymer is of great importance.

As our continuing research interest in DTT-based semiconducting polymers,[37, 38] we herein report the first synthesis of soluble homopolymers of 3-alkyl DTT and their application in OFETs. Instead of 3,5-dialkylated DTT,[36] 3-alkylated DTT was polymerized by oxidative polymerization and the regiorandom homopolymers (P3ADTT) thus obtained were used as active layer in organic thin film transistors. P3ADTT based OTFTs show an annealing-free hole mobility of up to 0.048 $cm^2/V \cdot s$ and current on/off ratio of 10^5 under ambient condition, which, to the best of our knowledge, is the highest hole mobility of regiorandom polymer semiconductors reported so far.

Experimental Section

Instrumentation and characterization

^{1}H NMR data were acquired on a Bruker DPX 400 MHz spectrometer. Gel permeation chromatography was carried out at 160 °C using a Polymer Labs PL 220 system using a refractive index detector and 1,2,4-trichlorobenzene as the eluent. UV-Vis-NIR spectra were recorded on a Shimadzu model 2501-PC. Differential scanning calorimetry (DSC) was carried out under nitrogen on a TA Instrument DSC Q100 instrument (scanning rate of 10 °C/min).

Material Synthesis

All reagents were used as received from Sigma-Aldrich. Monomers 3-tridecyldithieno[3,2-*b*:2',3'-*d*]thiophene (3ADTT-13) and 3-pentadecyldithieno[3,2-*b*:2',3'-*d*]thiophene (3ADTT-15) were synthesized according to the previously reported procedures[39] with slight modification (Scheme1): a mixture of 5-tridecyldithieno[3,2-b:2',3'-d]thiophene-2-carboxylic acid (4.23 g, 10 mmol) and quinolone (15 mL) was heated to 60 °C until turned to homogeneous. Copper power (630 mg, 10 mmol, 1 equivalent) was added while stirring and the mixture was heated to 220-230 °C. The reaction mixture was stirred for about 3 h until no gas bubble was observed. The mixture was slightly cooled down and passed through a short pad of celite. The celite pad was washed with hexane (200 mL). Combined organic solution was washed 10% HCl solution until it turned clear. The organic solution was then washed with water (3 × 100 mL), dried over anhydrous $MgSO_4$ and concentrated. The crude mixture was purified by flash chromatography using hexane as eluent and 3ADTT-13 was obtained as slightly yellow oil. ^{1}H NMR ($CDCl_3$, 400 MHz) 3ADTT-13: δ 7.35 (d, 1H), 7.29 (d, 1H), 6.99 (s, 1H), 2.73 (t, 2H), 1.77 (m, 2H), 1.25 (m, 20H), 0.88 (t, 3H).

ADTT-15 was synthesized from 5-pentadecyldithieno[3,2-*b*:2',3'-*d*]thiophene-2-carboxylic acid using same procedure as slightly yellow oil. ^{1}H NMR (CDCl3, 400 MHz) 3ADTT-15: δ 7.34 (d, 1H), 7.29 (d, 1H), 6.98 (s, 1H), 2.73 (t, 2H), 1.76 (m, 2H), 1.26 (m, 24H), 0.88 (t, 3H).

Synthesis of regiorandom homopolymers of 3ADTT by oxidative polymerization: Monomer 3ADTT-13 (1 equivalent) was dissolved in PhCl (0.033M). $FeCl_3$ (2.2 equivalent) was added while stirring and air was then gently bubbled into the reaction mixture. The mixture was slowly heated to 60 °C and stirred vigorously for 24 h. The reaction mixture was then poured into 200 mL EtOH and 10mL NH_3▪H2O and stirred overnight. The polymer was filtered and subjected to Soxhlet extraction with EtOH (24 h), hexanes (24 h), and chlorobenzene (24 h). The chlorobenzene fraction was then concentrated, precipitated into 200 mL of methanol, filtered and dried to obtain the final product as black solid (P3ADTT-13, 83% yield). P3ADTT-13: ^{1}H NMR (1,1,2,2-Tetrachloroethane-d_2, 70 °C) δ 7.45 (broad, ring proton), 3.02 (broad s, 1H, ring-CH_2, HT linkage), 2.81 (broad s, 1H, ring-CH_2, HH linkage), 1.83 (broad d, 2H), 1.6-1.1(20H), 0.92 (3H). GPC M_n = 12900, M_w = 32400.

P3ADTT-15 was obtained from 3ADTT-15 using same procedure as black solid (81% yield). P3ADTT-13: ^{1}H NMR (1,1,2,2-Tetrachloroethane-d_2, 70 °C) δ 7.45 (broad, ring proton), 3.03 (broad s, 1H, ring-CH_2, HT linkage), 2.80 (broad s, 1H, ring-CH_2, HH linkage), 1.82 (broad d, 2H), 1.8-1.1 (24H), 0.92 (3H). GPC M_n = 12200, M_w = 29700.

Cyclic voltammetry

Cyclic voltammetry experiments were performed using an Autolab potentiostat (model PGSTAT30) from Echochimie. The experiments were performed at room temperature in a glovebox with a conventional three electrode configuration consisting of a glass carbon working electrode, a platinum counter electrode, and a silver wire as a quasi-reference electrode. The electrolyte was 0.1 M tetrabutylammonium hexafluorophosphate in anhydrous acetonitrile. The polymer solution (2 mg·ml^{-1}in chlorobenzen) was drop cast onto the working electrode and dried under ambient conditions prior to measurements. Ferrocene was used as an internal standard for calculating the redox potentials of the samples following each batch of samples, and the ferrocene/ferrocenium redox couple was assumed to have an absolute value of 4.8 eV below the vacuum level.[40] The onset of the first oxidation peak was used to calculate the value of the HOMO.

OTFT device fabrication and characterization

The field effect transistor substrates were made using a heavily doped N-type silicon wafer as the common gate electrode and a 100 nm thermally oxidized SiO_2 layer as the gate dielectric. The gold source and drain electrodes were patterned in a bottom contact configuration using the conventional photolithography method. A 10 nm layer of titanium was used as an adhesion layer for the gold on SiO_2. We employed a ring-type geometry of source and drain electrodes, in order to eliminate the parasitic leakage path from source to drain. The SiO_2 surface of the wafer substrate was first cleaned with Piranha solution (mixture of 70% sulfuric acid and 30% hydrogen peroxide) and then modified with organosilane by immersing the clean wafer in 10mM hexane solution of octyltrichlorosilane (OTS-8) for45 minutes at room temperature, thoroughly rinsing the substrate with hexane and 2-isopropol then blowing dry with nitrogen gas. The gold source and drain electrodes were modified with octylthiol self-assembled monolayer to reduce the contact resistance. The substrate was immersed into 5 mM solution of octylthiol in ethanol for more than 24 hours, and then rinsed with ethanol before depositing the semiconductor layer.

A solution of P3ADTT, in chlorobenzene (4 mg·ml^{-1}) was deposited on the modified SiO_2 surface by drop-casting. The substrate was patterned with a series of transistors with various channel lengths (L) from 20μm to 100μm and widths (W) from 3 mm to 16 mm. Electrical properties of the transistors were characterized using a Cascade Microtech probe stationand an Agilent E5270B 8-Slot Precision Measurement Mainframe at ambient conditions without taking any precautions to isolate the material and device from exposure to ambient oxygen, moisture, or light. The OFET mobility was computed from the saturation region of the I-V curve with the relation:

$$I_{Dsat} = \frac{W}{2L} C_i \mu (V_g - V_{th})^2$$

Where I_{Dsat} is the drain current, μ is the field-effect mobility, C_i is the capacitance per unit area of the gate dielectric layer (SiO_2, 220 nm, C_i= 15.6 nF·cm^{-2}), and V_g and V_{th} are the gate voltage and threshold voltage respectively. V_{th} was derived from the relationship between the square root of I_{Dsat} at the saturated regime and V_g by extrapolating the measured data to I_{Dsat}= 0.

Design and Synthesis

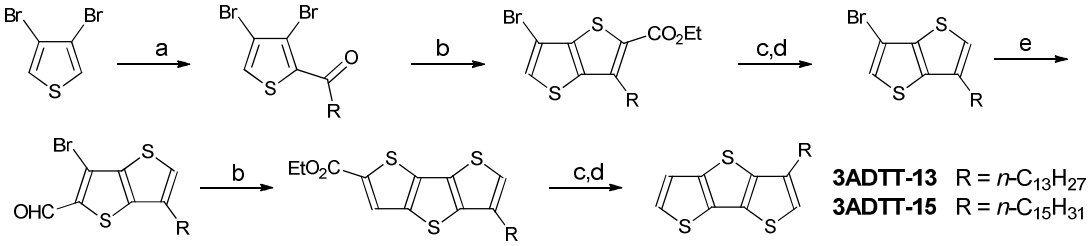

Scheme 1 Synthesis of the monomer 3ADTT. Conditions: (a) tetradecanoyl chloride or palmitoyl chloride, $AlCl_3$, CH_2Cl_2, 0 °C; (b) K_2CO_3, ethyl mercaptoacetate, DMF, 60 °C; (c) LiOH, H_2O/THF/MeOH, reflux, then acidified; (d) Cu, Quinoline, 220-230 °C; (e) LDA, THF, 0 °C , then 1-formylpiperidine.

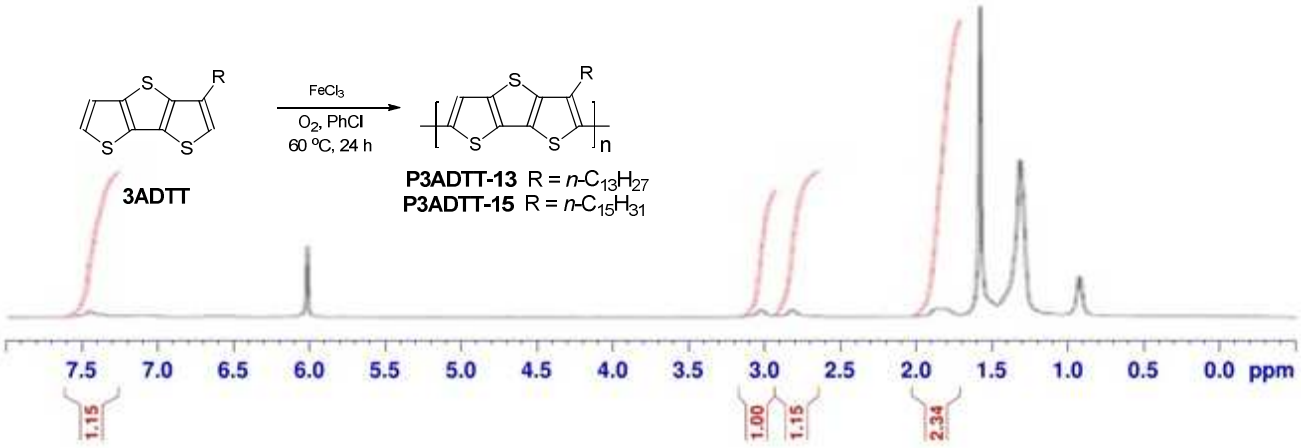

Fig. 1 Synthesis of regiorandom homopolymer P3ADTT and ^{1}H NMR spectrum of P3ADTT-13 in 1,1,2,2-tetrachloroethane-d_2 at 70 °C.

Poly(3,5-didecanyldithieno[3,2-*b*:2',3'-*d*]thiophene), reported by Zhang et al., shows absorption maximum in near-UV range (about 380 nm) and has high onset oxidation potential of 1.76 V versus Ag^+/Ag.[36] We envision that introduction of two alkyl chain at both 3 and 5 positions of DTT ring will lead to strong head-to-head side-chain interaction and big dihedral angles for the polymer backbone. The less coplanar polymer structure is unfavourable for π delocalization, interchain π-π stacking and thus charge-transfer ability.[41, 42] From this point of view, monosubstituted DTT, 3-alkyldithieno[3,2-*b*:2',3'-*d*]thiophene (3ADTT), should be a more promising building block to facilitate the charge-transfer. But compared with *n*-hexyl side chain commonly used in soluble poly(3-alkylthiophene), longer side chain needs to be introduced into the 3-position of DTT ring in order to maintain sufficient solubility for both DTT-based monomer and homopolymer. Thus two monomers 3ADTT-13 and 3ADTT-15, containing *n*-tridecyl (*n*-$C_{13}H_{27}$) and *n*-pentadecyl (*n*-$C_{15}H_{31}$) side chain respectively, were synthesizedfrom 3,4-dibromothiophene to evaluate side chain effect (See Scheme 1). Under similar condition for the polymerization of 3-alkylthiophene,[43] 3ADTT was directly polymerized via oxidative polymerization using Iron(III) Chloride and oxygen as oxidants in chlorobenzene at 60 °C (See equation in Fig. 1). After Soxhlet extraction process, regiorandom homopolymers P3ADTT-13 and P3ADTT-15 were obtained from chlorobenzene fraction in over 80% yields as dark blue solids. From the ^{1}H NMR spectra of the polymer (Fig. 1), two peaks with almost equal integration were observed at 3.02 ppm and 2.81 ppm, which are assigned as the HT linkage and HH linkage ring-CH_2 respectively, indicating the regiorandom nature of the P3ADTT homopolymers.

Characterization

Optical characterization

Solution and thin film UV-Vis absorption for P3ADTT-13 and P3ADTT-15 were measured as shown in Fig. 1. Absorption curves for P3DTT-13 and P3ADTT-15 in solution are almost identical with maximum absorption peak at λ_{max} = 460 nm, which is similar with regioregular P3HT (456 nm) but largely red-shifted relative to that of regiorandom P3HT (428 nm).[12] This phenomenon suggested that regiorandom P3ADTT

polymer, compared with regiorandom P3HT, have more extensive π-conjugation among polymer chain in solution phase, due to extended π-conjugation of fused thiophene rings of DTT moiety. In thin film spectra, weak additional shoulder appears at around 600 nm and maximum absorption peak appears at 503 nm with 43 nm red-shift relative to that of solution spectra, indicating a higher structural ordering in solid state. As comparison, absorption maximum of regiorandom P3HT thin film is 438 nm with only 10 nm red-shift relative to that of solution spectra and no additional shoulder was observed, which proved that planarity expansion from thiophene to DTT can indeed lead to enhanced interchain π-π stacking (see Table 1 for the comparison).

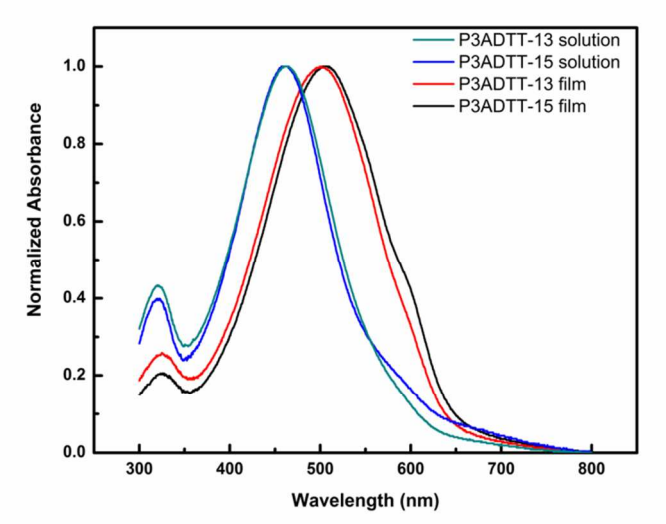

Fig. 2 UV-Vis absorption spectra for P3ADTT: as-casting thin film spectra (red and black line); chloroform solution spectra (blue and green line).

Table 1 Comparison of UV-Vis and fluorescence data of regiorandom P3ADTT-13, regiorandom P3HT and regioregular P3HT.[a]

	λ_{max} – Solution (nm)	λ_{max} – Film (nm)	$f(\lambda)_{max}$ (nm)
Regiorandom**P3ADTT-13**	460	503[b]	540
RegiorandomP3HT	428	438	550
Regioregular P3HT	456	526, 556, 610	570

[a]Refer to reference [12] for the data of P3HT. [b]Weak shoulder at 600 nm.

Electrochemical characterization

Cyclic voltammetric (CV) measurement of P3ADTT thin film was carried out by three-electrode cell in 0.1 M tetrabutylammonium hexafluorophosphate solution in anhydrous acetonitrile using ferroncene/ferrocenium couple as internal reference. P3ADTT-13 and P3ADTT-15 both showed reversible oxidation and reduction curve and had almost identical oxidation onset potentials of around 0.34V *vs.* Fc/Fc^+(Fig. 3). Thus the HOMO level estimated from oxidation onset potential is around -5.14 eV, which is 0.24 eV deeper than that of regioregular P3HT (-4.9 eV) measured under the same condition. With such lower lying HOMO, P3ADTT-13 **and P3ADTT-15 are** expected to have improved oxidation stability than P3HT.

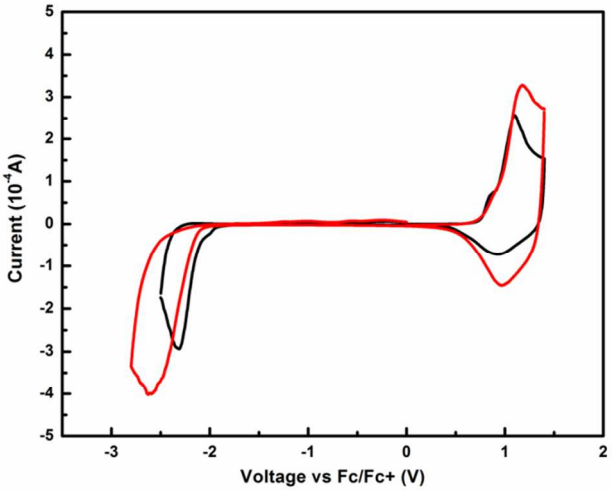

Fig. 3 Voltammetric curves of P3ADTT thin-films: P3ADTT-13 (black line) and P3ADTT-15 (red line).

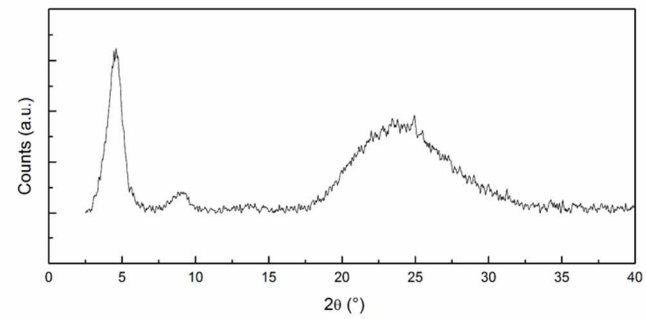

Fig. 4 XRD characterization of P3ADTT-13 film.

Crystallinity and morphologycharacterization

Fig. 4 shows the X-ray diffraction pattern for an as-cast thin film of P3ATT-13 in chlorobenzene. Strong primary diffraction peak at 2θ = 4.6° and weak second order peak at 9.2° were observed, which corresponds to an inter-chain *d* spacing of 19.1 Å. Moreover, prominent π-π stacking peak was observed at 2θ = 24.0°, indicating a short π-π stacking distance of 3.7 Å. The XRD result indicates that the non-annealed P3ATT-13 film exhibited some degree of ordering and contained both face-on and edge-on orientations. Differential scanning calorimetry (DSC) was carried out for P3ADTT-13 to investigate its thermal property (Fig. 5). No noticeable endothermic peak upon heating or exothermic peak upon cooling was observed between

0 °C to 350 °C. The absence of side chain melting indicated the weak interlayer side chain interaction in P3ADTT-13, which should be due to its regiorandom nature. And the backbone melting peak should appear higher than 350°C based on the relatively strong interchain backbone interaction indicated by XRD analysis.[44] The semi-crystalline structure of P3ATT-13 film is remarkably different with the disordered and amorphous structure of regiorandom P3HT film, which shows no peak in the XRD spectra even after thermal annealing.[45] This phenomenon revealed that planarity expansion of core unit from single thiophene ring to DTT can indeed led to better structural order in the polymer film. Atomic force microscopy (AFM) was then used to investigate the surface morphology. The AFM image showed clear fibrillar features, which is favoured for charge transfer. (Fig. 6)

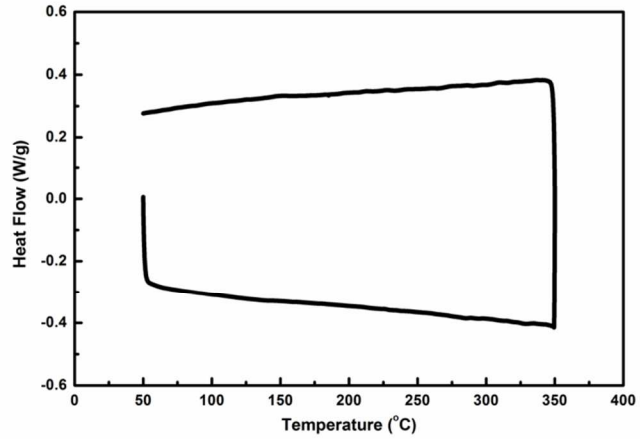

Fig. 5 DSC curve showing the heating/cooling cycle for P3ADTT-13. The samples were heated from 50 °C to 350 °C and back to 50 °C at a ramp rate of 10 °C·min^{-1}.

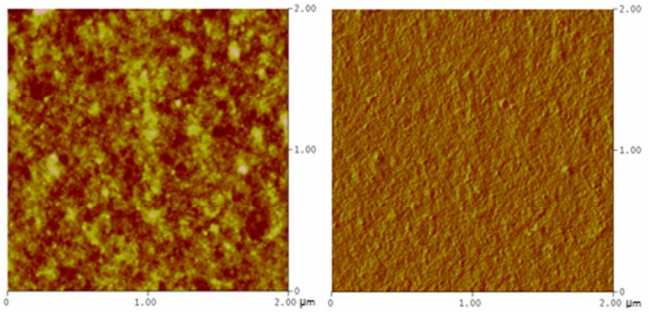

Fig. 6 AFM height image of P3ADTT-13 film.

TFT Characterization

Differential Bottom-gate, bottom-contact TFT devices using P3ADTT as semiconducting layer was fabricated to investigate the charge transfer ability of P3ADTT. The devices were built on an n-doped silicon wafer with octyltrichlorosilane-modified SiO_2 gate dielectric and octylthiol-modified gold source/drain electrodes. Fig. 5 shows the typical output curve and transfer characteristics of a representative as-prepared TFT device based on P3ADTT-13 (W/L = 4000/120) with no post-deposition thermal annealing under ambient conditions. The output characteristics display very good saturation behaviour with no obvious contact resistance. The transfer characteristics show a field-effect hole transporting characteristic with near-zero turn-on voltage and a threshold voltage of -15 V. The mobility estimated at the saturated regime is 0.048 cm^2/V·s with a current on/off ratio of more than 10^5. Moreover, due to the deeper HOMO level and thus improved oxidation stability of P3ADTT, device fabrication and mobility measurement were all carried out in ambient conditions without taking any precautions to prevent exposure to ambient oxygen and light. OTFT device based on P3ADTT-15 showed almost identical hole transporting characteristic with device based on P3ADTT-13, indicating that change the side chain from *n*-tridecyl to *n*-pentadecyl has negligible impact on charge transfer property. The mobility of this regiorandom P3ADThomopolymer film was much higher than that of regiorandom P3HT (10^{-4} cm^2/V·s)[10] and comparable to that of regioregular P3HT (0.05-0.1 cm^2/V·s)[15] measured under inert atmosphere. The better structural order of P3ADTT-13 film observed by XRD and the fibrillar features observed by AMF should be the origin of its significantly improved charge transfer mobility. No significant change in the saturation hole mobility was observed after thermal annealing of the OTFT devices at temperature up to 140 °C. This is consistent with DSC result that P3ADTT film hadthe weak interlayer side-chain interactions and exhibited no crystalline improvement after thermal treatment.[44]As comparison, the mobility of both regiorandom and regioregular P3HT is decreased after thermal annealing treatment.[10] Since post-deposition thermal annealing process is quite time-consuming and energy-intensive, the annealing–free characteristic of P3ADTT homopolymer makes it a promising OTFT channel semiconductor for a variety of electronic applications.

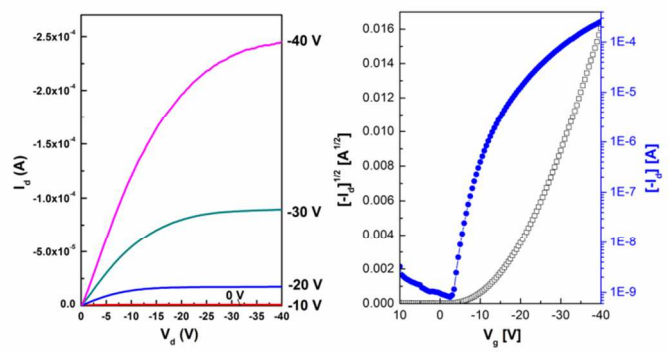

Fig. 7 I-V characteristics of an illustrative TFT device using P3ADTT-13 semiconductor: (a) output curves at different gate voltages; (b) transfer curve in saturated regime at constant.

The annealing-free nature of P3ADTT based transistor intrigued us to investigate the device performance at elevated temperature. To our delight, the OTFT device fabricated by P3ADTT-13 displayed much better thermal stability than that of P3HT (Fig. 8). We found that hole mobility of P3ADTT-13 film increased as the device was heated up while the current on/off ratio remained at more than 10^5. This observation is consistent with traditional hopping model and the increased mobility should be due to the higher charge carrier

concentration at elevated temperature. The highest hole mobility (0.13 $cm^2/V \cdot s$) was observed at about 160 °C and this high mobility could be maintained up to 200 °C. In contrast, the mobility of P3HT film decreases dramatically with temperature due to the formation of conformation defects in the polymer chain which will inhibit the charge transportation.[10, 46] This phenomenon further proved that planarity expansion of core unit from thiophene to DTT can not only promote the polymer interchain π-π stacking in solid state but also make the polymer film less liable to undergo unfavourable morphology transition at elevated temperature.

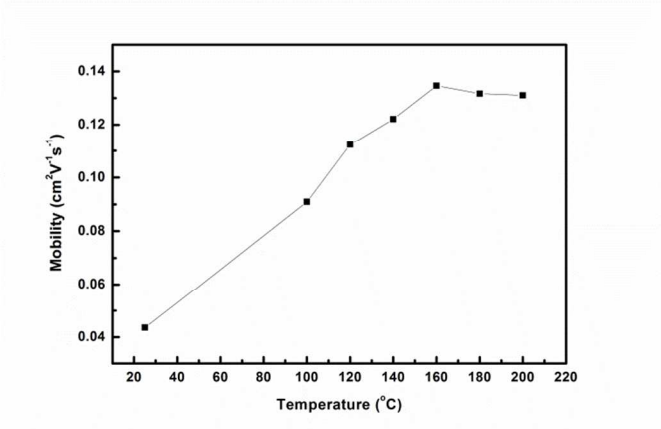

Fig. 8 Hole mobility of P3ADTT-13 film at different temperature.

Conclusions

We have synthesized the first regiorandom homopolymer based on 3-alkyldithieno[3,2-*b*:2',3'-*d*]thiophene (P3ADTT) and investigated its application in organic field-effect transistor. Compared with its analogue polymer – P3HT, P3ADTT homopolymer exhibits better self-assembly, enhanced oxidation stability and thermal stability, much higher charge transfer ability (0.048 $cm^2/V \cdot s$) and current on/off ratio (greater than 10^5) in OTFT devices. To the best of our knowledge, the hole mobility of P3ADTT we discovered is the highest mobility reported for random polymers so far. The easy accessibility and convenient solution/post-annealing-free processability make P3ADTT promising candidate for low-cost printable electronic fabrication. Further investigation on the application of P3ADTT in OTFT and OPV devices and usage of DTT as building block for the construction of useful organic semiconducting polymers will be reported in due course.

Notes

[a]Institute of Materials Research and Engineering (IMRE), Agency for Science,Technology, and Research (A*STAR), 3 Research Link, Singapore, 117602. E-mail: j-li@imre.a-star.edu.sg; Fax: +6567741042; Tel:+6568747116

[b] Department of Physics, La Trobe University, Bundoora, Victoria 3086 , Australia.

References

1. A. C. Arias, J. D. MacKenzie, I. McCulloch, J. Rivnay and A. Salleo, *Chem. Rev.* , 2010, **110**, 3-24.
2. A. Facchetti, *Chem. Mater.* , 2010, **23**, 733-758.
3. C. J. Brabec, S. Gowrisanker, J. J. M. Halls, D. Laird, S. Jia and S. P. Williams, *Adv. Mater.* , 2010, **22**, 3839-3856.
4. Y.-J. Cheng, S.-H. Yang and C.-S. Hsu, *Chem. Rev.* , 2009, **109**, 5868-5923.
5. H. Zhou, L. Yang and W. You, *Macromolecules*, 2012, **45**, 607-632.
6. G. Li, R. Zhu and Y. Yang, *Nat Photon*, 2012, **6**, 153-161.
7. S. Allard, M. Forster, B. Souharce, H. Thiem and U. Scherf, *Angew. Chem. Int. Ed.* , 2008, **47**, 4070-4098.
8. H. Klauk, *Chem. Soc. Rev.* , 2010, **39**, 2643-2666.
9. L. Biniek, B. C. Schroeder, C. B. Nielsen and I. McCulloch, *J. Mater. Chem.* , 2012, **22**, 14803-14813.
10. A. Assadi, C. Svensson, M. Willander and O. Inganäs, *Appl. Phys. Lett.* , 1988, **53**, 195-197.
11. Z. Bao, A. Dodabalapur and A. J. Lovinger, *Appl. Phys. Lett.* , 1996, **69**, 4108-4110.
12. T.-A. Chen, X. Wu and R. D. Rieke, *J. Am. Chem. Soc.* , 1995, **117**, 233-244.
13. R. D. McCullough, *Adv. Mater.* , 1998, **10**, 93-116.
14. R. D. McCullough, R. D. Lowe, M. Jayaraman and D. L. Anderson, *J. Org. Chem.*, 1993, **58**, 904-912.
15. H. Sirringhaus, P. J. Brown, R. H. Friend, M. M. Nielsen, K. Bechgaard, B. M. W. Langeveld-Voss, A. J. H. Spiering, R. A. J. Janssen, E. W. Meijer, P. Herwig and D. M. de Leeuw, *Nature*, 1999, **401**, 685-688.
16. M. S. A. Abdou, F. P. Orfino, Y. Son and S. Holdcroft, *J. Am. Chem. Soc.* , 1997, **119**, 4518-4524.
17. M. L. Chabinyc, M. F. Toney, R. J. Kline, I. McCulloch and M. Heeney, *J. Am. Chem. Soc.* , 2007, **129**, 3226-3237.
18. H. H. Fong, V. A. Pozdin, A. Amassian, G. G. Malliaras, D.-M. Smilgies, M. He, S. Gasper, F. Zhang and M. Sorensen, *J. Am. Chem. Soc.* , 2008, **130**, 13202-13203.
19. I. McCulloch, M. Heeney, C. Bailey, K. Genevicius, I. MacDonald, M. Shkunov, D. Sparrowe, S. Tierney, R. Wagner, W. Zhang, M. L. Chabinyc, R. J. Kline, M. D. McGehee and M. F. Toney, *Nat. Mater.* , 2006, **5**, 328-333.
20. M. He, J. Li, M. L. Sorensen, F. Zhang, R. R. Hancock, H. H. Fong, V. A. Pozdin, D.-M. Smilgies and G. G. Malliaras, *J. Am. Chem. Soc.* , 2009, **131**, 11930-11938.
21. M. He, J. Li, A. Tandia, M. Sorensen, F. Zhang, H. H. Fong, V. A. Pozdin, D.-M. Smilgies and G. G. Malliaras, *Chem. Mater.* , 2010, **22**, 2770-2779.
22. T. Ozturk, E. Ertas and O. Mert, *Tetrahedron*, 2005, **61**, 11055-11077.
23. X.-C. Li, H. Sirringhaus, F. Garnier, A. B. Holmes, S. C. Moratti, N. Feeder, W. Clegg, S. J. Teat and R. H. Friend, *J. Am. Chem. Soc.* , 1998, **120**, 2206-2207.
24. Y. M. Sun, Y. Q. Ma, Y. Q. Liu, Y. Y. Lin, Z. Y. Wang, Y. Wang, C. A. Di, K. Xiao, X. M. Chen, W. F. Qiu, B. Zhang, G. Yu, W. P. Hu and D. B. Zhu, *Adv. Funct. Mater.* , 2006, **16**, 426-432.
25. S. Zhang, Y. Guo, L. Wang, Q. Li, K. Zheng, X. Zhan, Y. Liu, R. Liu and L.-J. Wan, *The Journal of Physical Chemistry C*, 2009, **113**, 16232-16237.
26. B. Balan, C. Vijayakumar, A. Saeki, Y. Koizumi, M. Tsuji and S. Seki, *Polymer Chemistry*, 2013, **4**, 2293-2303.
27. Q. Bao, J. Li, C. M. Li, Z. L. Dong, Z. Lu, F. Qin, C. Gong and J. Guo, *The Journal of Physical Chemistry B*, 2008, **112**, 12270-12278.
28. X. Huang, C. Zhu, S. Zhang, W. Li, Y. Guo, X. Zhan, Y. Liu and Z. Bo, *Macromolecules*, 2008, **41**, 6895-6902.
29. K. Lu, C.-a. Di, H. Xi, Y. Liu, G. Yu, W. Qiu, H. Zhang, X. Gao, Y. Liu, T. Qi, C. Du and D. Zhu, *J. Mater. Chem.* , 2008, **18**, 3426-3432.
30. Y. Song, W. Zhang, W. Zhang, J. Li, S. Li, H. Zhou and J. Qin, *Chem. Lett.* , 2007, **36**, 1206-1207.

31. X. Zhan, Z. a. Tan, B. Domercq, Z. An, X. Zhang, S. Barlow, Y. Li, D. Zhu, B. Kippelen and S. R. Marder, *J. Am. Chem. Soc.* , 2007, **129**, 7246-7247.
32. J. Li, F. Qin, C. M. Li, Q. Bao, M. B. Chan-Park, W. Zhang, J. Qin and B. S. Ong, *Chem. Mater.* , 2008, **20**, 2057-2059.
33. J. W. Jung, F. Liu, T. P. Russell and W. H. Jo, *Energy Environ. Sci.* , 2012, **5**, 6857-6861.
34. M. Biserni, A. Marinangeli and M. Mastragostino, *J. Electrochem. Soc.* , 1985, **132**, 1597-1601.
35. P. Dimarco, M. Mastragostino and C. Talianic, *Mol. Cryst. Liq. Cryst.*, 1985, **118**, 241-244.
36. S. Zhang, H. Fan, Y. Liu, G. Zhao, Q. Li, Y. Li and X. Zhan, *J. Polym. Sci., Part A: Polym. Chem.* , 2009, **47**, 2843-2852.
37. J. Li, K.-H. Ong, S.-L. Lim, G.-M. Ng, H.-S. Tan and Z.-K. Chen, *Chem. Commun.* , 2011, **47**, 9480-9482.
38. J. Li, H.-S. Tan, Z.-K. Chen, W.-P. Goh, H.-K. Wong, K.-H. Ong, W. Liu, C. M. Li and B. S. Ong, *Macromolecules*, 2011, **44**, 690-693.
39. M. He and F. Zhang, *J. Org. Chem.*, 2006, **72**, 442-451.
40. J. Pommerehne, H. Vestweber, W. Guss, R. F. Mahrt, H. Bässler, M. Porsch and J. Daub, *Adv. Mater.* , 1995, **7**, 551-554.
41. R. M. S. Maior, K. Hinkelmann, H. Eckert and F. Wudl, *Macromolecules*, 1990, **23**, 1268-1279.
42. X. Zhang, M. Köhler and A. J. Matzger, *Macromolecules*, 2004, **37**, 6306-6315.
43. K. Yoshino, S. Nakajima, M. Onoda and R. Sugimoto, *Synth. Met.* , 1989, **28**, 349-357.
44. H. Pan, Y. Wu, Y. Li, P. Liu, B. S. Ong, S. Zhu and G. Xu, *Adv. Funct. Mater.* , 2007, **17**, 3574-3579.
45. K. Kanai, T. Miyazaki, H. Suzuki, M. Inaba, Y. Ouchi and K. Seki, *PCCP* 2010, **12**, 273-282.
46. A. Zen, J. Pflaum, S. Hirschmann, W. Zhuang, F. Jaiser, U. Asawapirom, J. P. Rabe, U. Scherf and D. Neher, *Adv. Funct. Mater.* , 2004, **14**, 757-764.